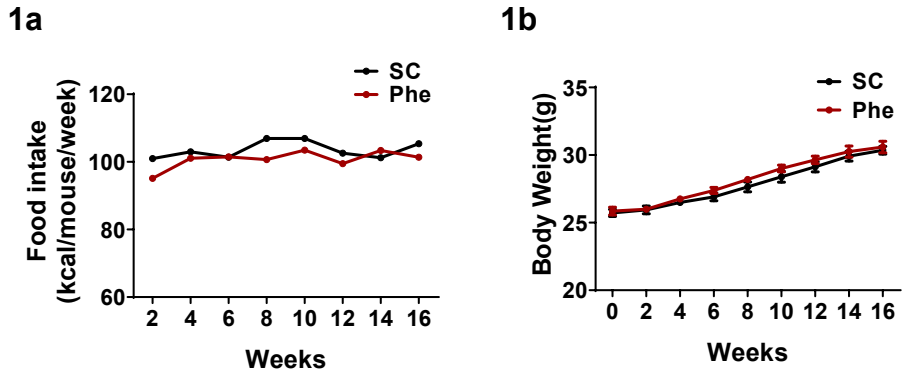

Extended Data Fig. 1 Phenylalanine-supplemented chow induced symptoms of type 2 diabetes in mice, related to Fig. 1

1a-1b, **Phe-chow had negligible effects on mouse food intake and body weights.** The food intake (**1a**) and body weight (**1b**) of SC- and Phe- chow-fed male mice were monitored during treatments.

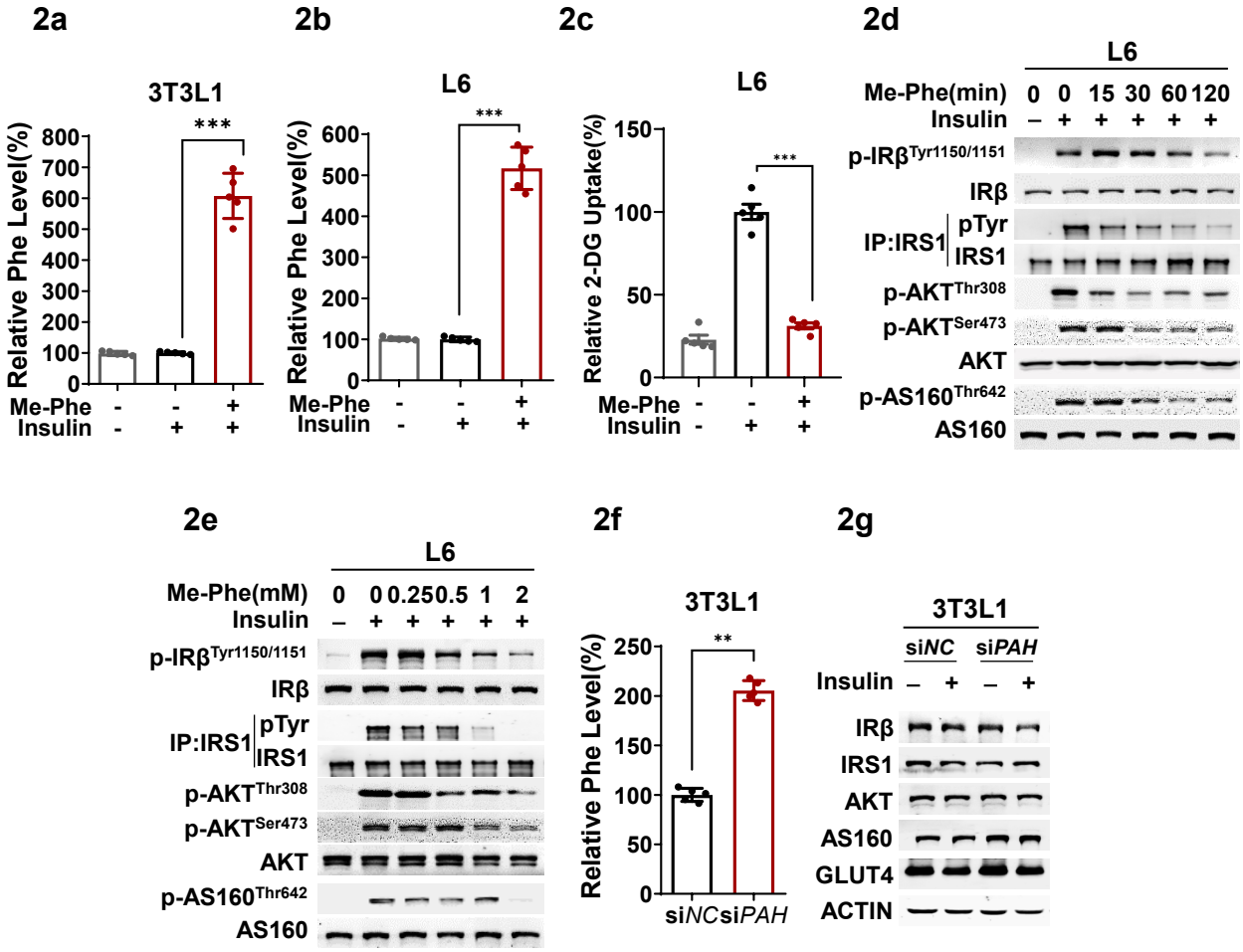

Extended Data Fig. 2 Intracellular phenylalanine blocked insulin signaling in cultured cells, related to Fig. 1

2a-2b, Me-Phe treatment elevated intracellular phenylalanine levels. Relative intracellular phenylalanine levels were measured by LC-MS for 3T3-L1 adipocytes (**2a**) and L6 myocytes (**2b**) that were cultured in the presence and absence of Me-Phe in the culture media. (n = 5).

2c, Me-Phe treatment decreased 2-DG uptake in L6 myocytes. The 2-DG uptake of L6 cells was detected in the presence and absence of Me-Phe in the culture media. (n = 5).

2d-2e, Me-Phe treatment impaired insulin signaling in L6 myocytes. The time- (**2d**) and dose-dependent (**2e**) effects of Me-Phe on the phosphorylation of IR, IRS1, AKT and AS160 in L6 myocytes were detected.

2f, PAH knockdown increased intracellular phenylalanine levels. Relative intracellular phenylalanine levels of 3T3-L1 adipocytes and in siPAH 3T3-L1 adipocytes were compared (n = 5).

2g, PAH knockdown did not alter the protein levels of components of insulin signaling. IR, IRS1, AKT, AS160 and GLUT4 protein levels in siNC and siPAH 3T3-L1 adipocytes were detected.

2h, Me-Tyr treatment increased phenylalanine levels. Relative intracellular phenylalanine levels of untreated and Me-Tyr-treated 3T3-L1 adipocytes were detected by LC-MS (n = 5).

Values are expressed as the mean ± SEM. *p < 0.05, **p < 0.01, ***p < 0.001, hereafter for measurements in supplementary figures.

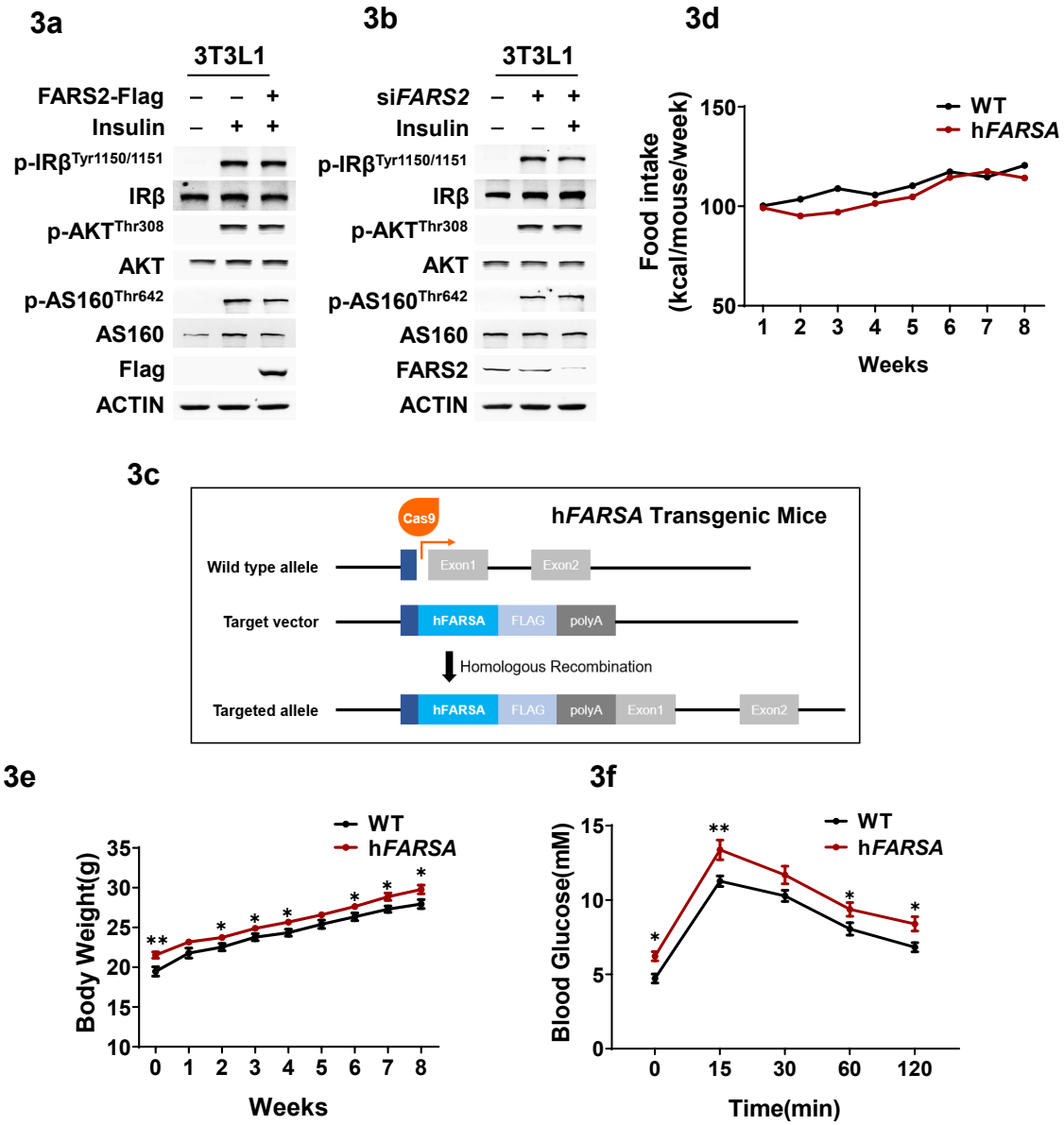

Extended Data Fig. 3 FARS, but not FARS2 overexpression, blunted insulin signaling, related to Fig. 2.

3a, FARS2 overexpression did not impair insulin signaling. Phosphorylation of IR, AKT, and AS160 in 3T3-L1 adipocytes and 3T3-L1 adipocytes overexpressing FARS2 was measured.

3b, FARS2 silencing had a negligible impact on insulin signaling. Phosphorylation of components of the insulin signaling pathway was detected in 3T3-L1 adipocytes and 3T3-L1 adipocytes with FARS2 silencing.

3c, Generation of hFARSA-transgenic mice. A schematic diagram is shown of the strategy to generate hFARSA-transgenic mice.

3d-3e, Physiologies of hFARSA-transgenic mice. Food intake (**3d**) and body weights (**3e**) of C57 and hFARSA-transgenic C57 mice were monitored (WT, n = 9, hFARSA-transgenic, n= 10 mice).

3f, hFARSA-transgenic mice developed glucose intolerance. Glucose tolerance tests were performed for fasted 8-week-old hFARSA-transgenic mice (WT, n = 9, hFARSA-transgenic, n= 10 mice).

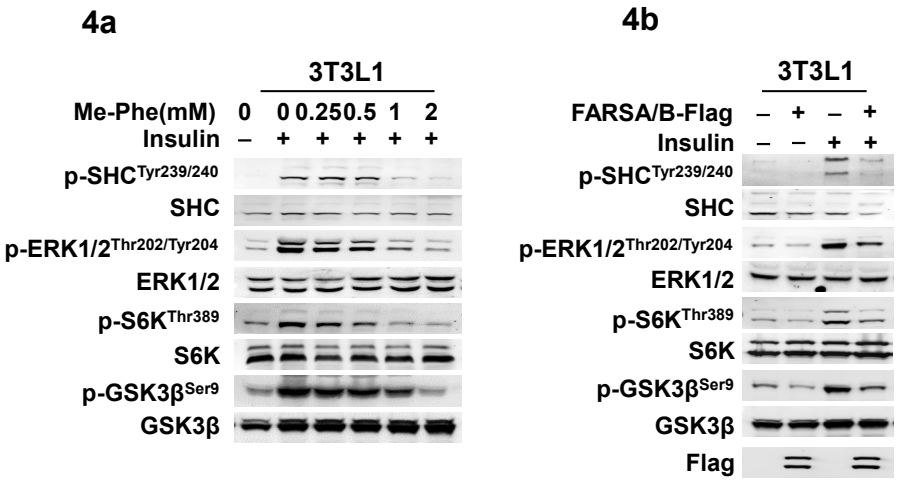

Extended Data Fig. 4 Me-Phe treatment and FARSA/B overexpression inhibited the phosphorylation of noninsulin signaling IR targets, related to Fig. 3.

4a-4b, The phosphorylation of SHC, ERK1/2, S6K and GSK3β in 3T3-L1 adipocytes and Me-Phe-treated (**4a**) or FARSA/B-overexpressing (**4b**) 3T3-L1 adipocytes was detected.

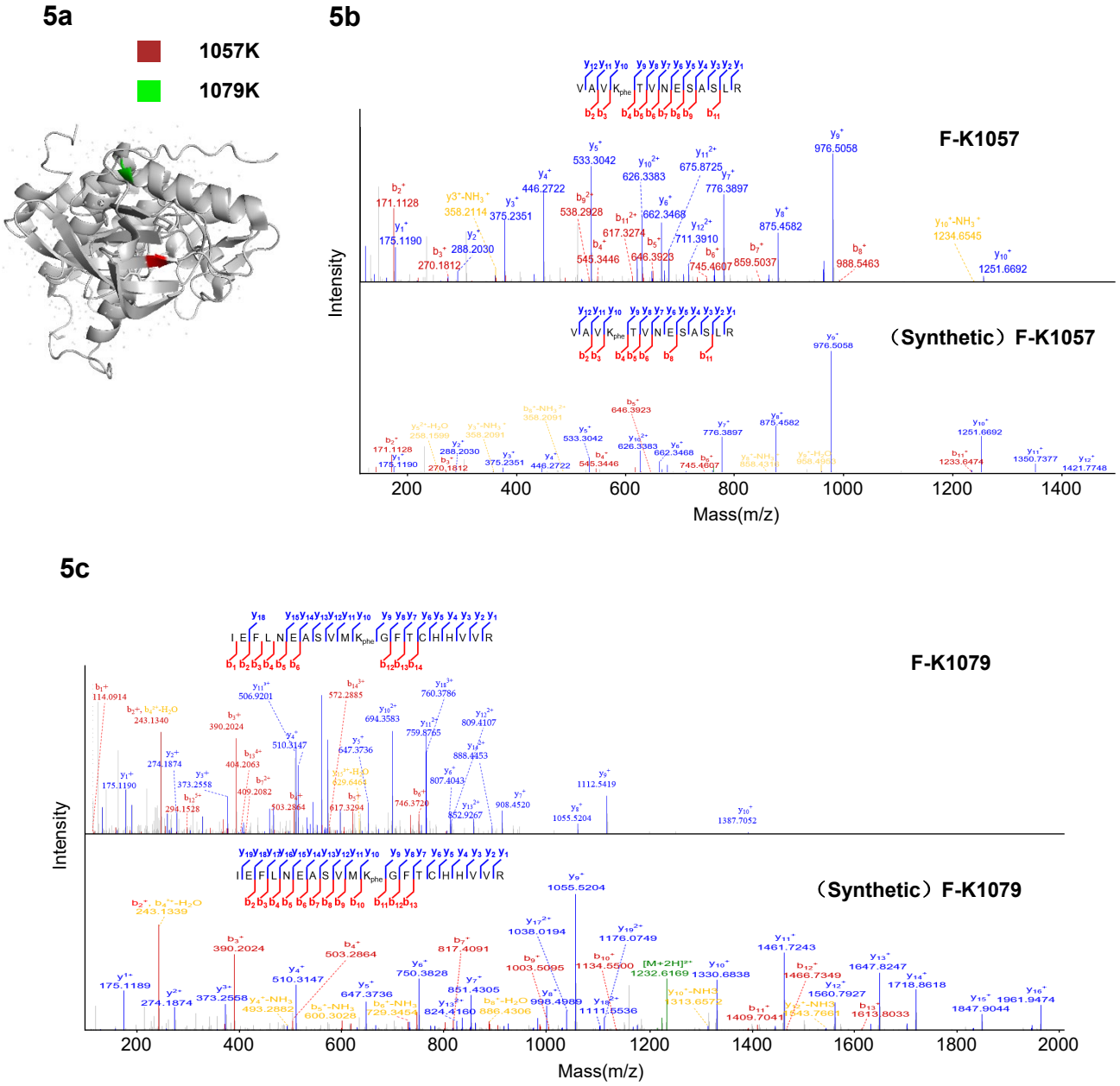

Extended Data Fig. 5 FARS phenylalanylated Lys1079 and Lys1057 of IR, related to Fig. 3.

5a, K1057 and K1079 are on the surface of IRβ. PyMol simulation showed that K1057 (red) and K1079 (green) are located at the surface of the IRβ protein (PDB: 5hhw).

5b-5c, **MS identification and confirmation of F-K1057 and F-K1079**. The MS/MS spectra that identified K1057 (**5b**) and K1079 (**5c**) were phenylalanylated and matched the MS/MS spectra from synthetic Y-K1057 and Y-K1079 peptides (lower, **5b** and **5c**).

5d-5e, **Characterization of site-specific F-K1057 and F-K1079 antibodies**. F-K1057 (**5d**) and F-K1079 (**5e**) site-specific antibodies were tested for their reactivity to F-K1057- and F-K1079-containing peptides (TRVAVK$_{1057phe}$TVNES and EASVMK$_{1079phe}$GFTCH) and peptides with the same amino acid sequences devoid of phenylalanylated lysine.

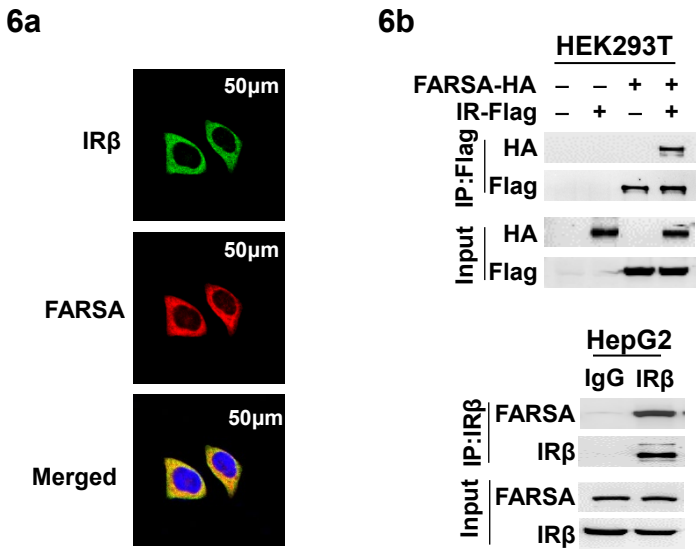

Extended Data Fig. 6 FARSA interacted with IR, related to Fig. 3.

6a, FARSA colocalized with IRβ. Immunofluorescence staining of IRβ (green) and FARSA (red) in HepG2 cells is shown.

6b, **FARSA interacted with IRβ**. A coimmunoprecipitation assay showed that ectopically expressed (upper) and endogenous (lower) FARSA interacted with IRβ in HepG2 cells.

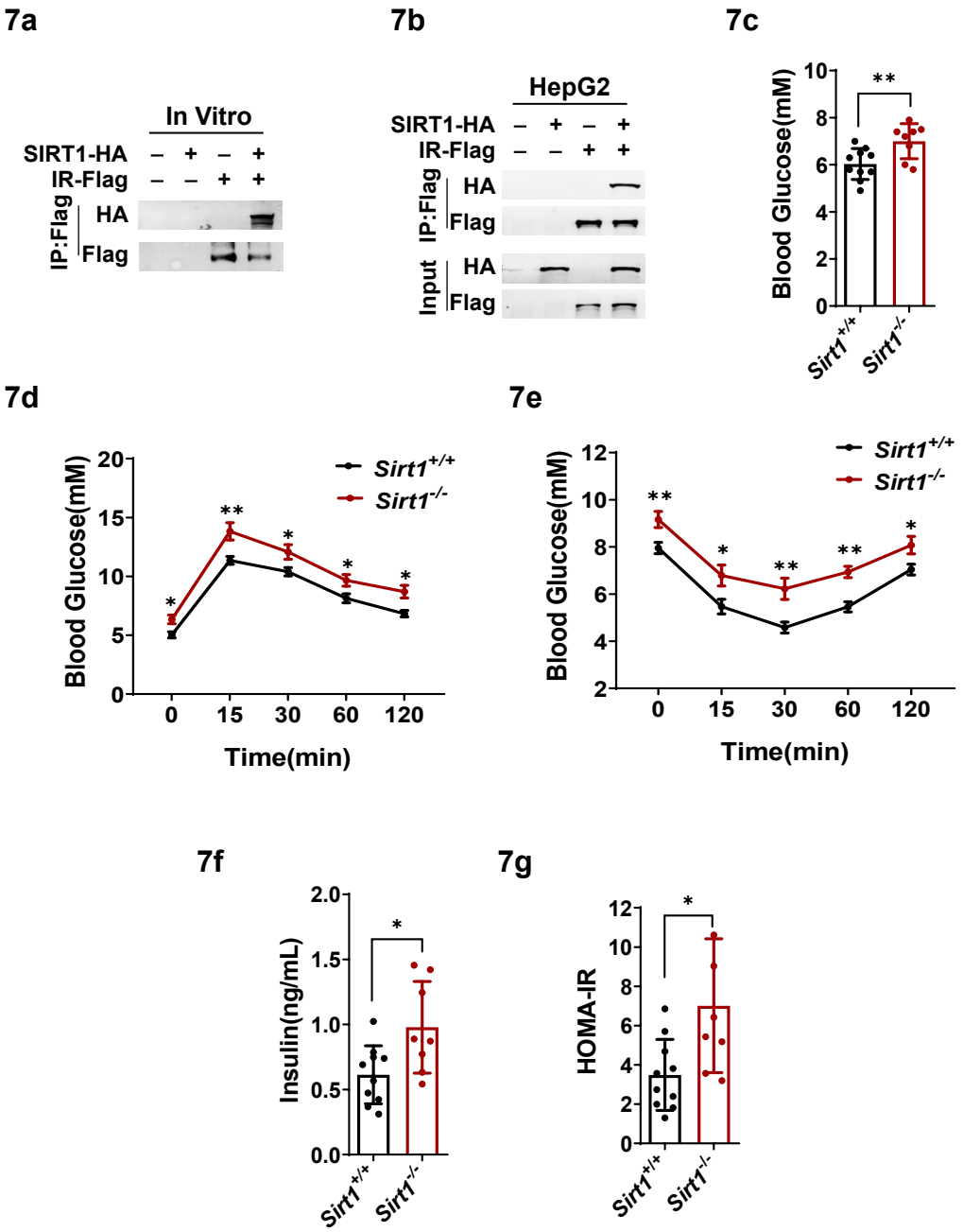

Extended Data Fig. 7 SIRT1 removed F-K1057 and F-K1079 and sensitized insulin signaling, related to Fig. 5.

7a-7b, SIRT1 interacted with IRβ. Recombinant SIRT1 pulled down IRβ (**7a**) and ectopically expressed SIRT1 coimmunoprecipitated with overexpressed IRβ in HEK293T cells (**7b**).

7c-7g, *Sirt1* knockout induced T2D symptoms. Blood glucose levels of 4-week-old (**7c**) and 8-week-old mice (**7d**), insulin tolerance (**7e**), blood insulin levels (**7f**), and HOMA-IR values (**7g**) of fasted wild-type (n = 10) and *Sirt*$^{-/-}$ (n = 8) C57 mice were measured.

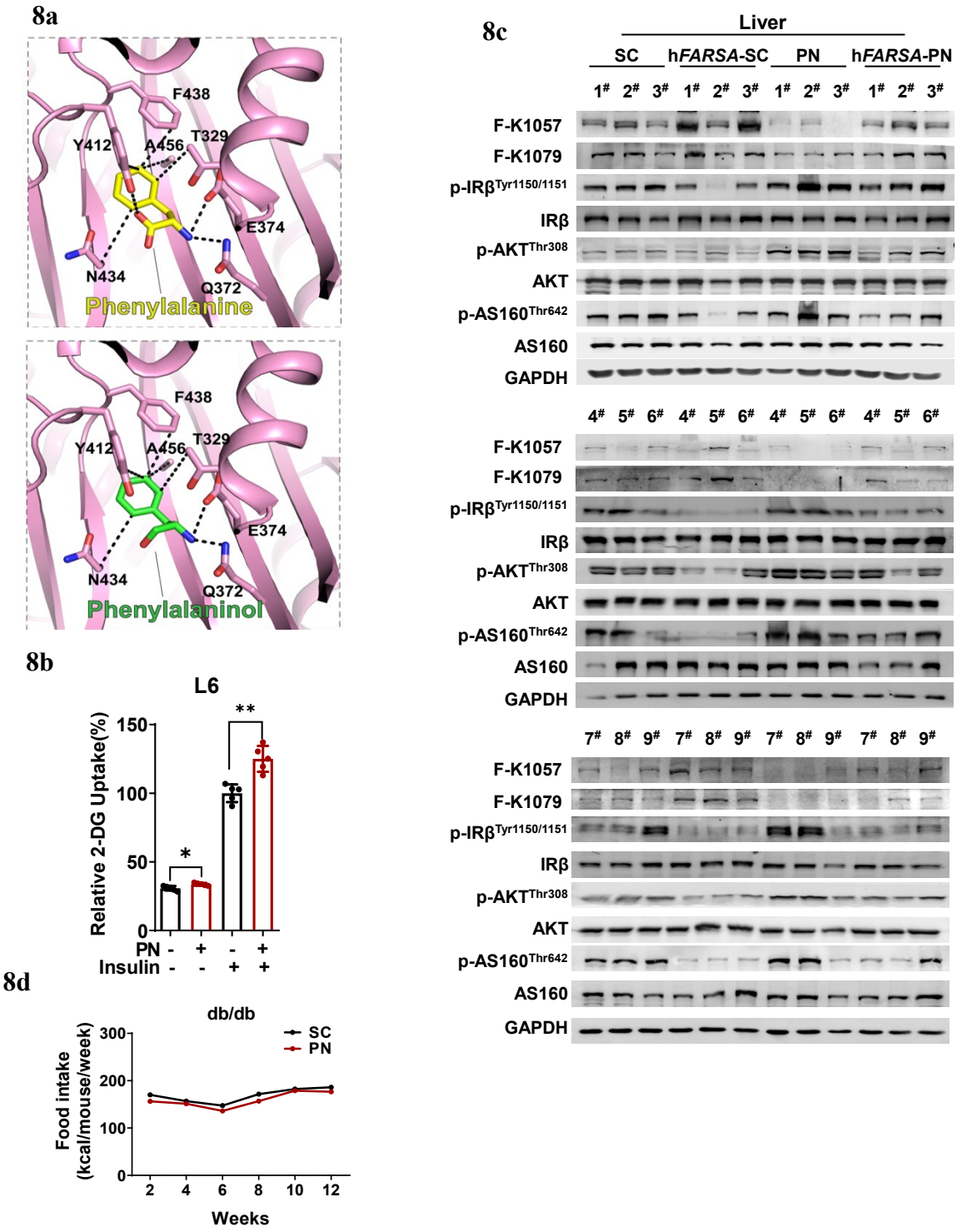

Extended Data Fig. 8 Decreasing F-K1057 and F-K1079 restored insulin signaling, related to Fig. 7

8a, **Phenylalaninol occupied the phenylalanine binding pocket of FARSA**. Projected detailed interactions between phenylalanine, phenylalaninol and FARSA were illustrated.

8b, **Phenylalaninol treatment improved glucose uptake by L6 myocytes**. The effects of phenylalaninol on 2-DG uptake by L6 cells were measured in the absence and presence of insulin treatments. (n = 5)

8c, Phenylalaninol decreased F-K1057 and F-K1079 levels and relieved diabetic symptoms in *hFARSA*-transgenic mice. Original western blot results of **Fig. 7e**.

8d, Phenylalaninol did not affect the food intake of db/db mice. Food intake of db/db mice fed standard chow (n=10) and phenylalaninol-supplemented chow (n=10) was monitored over time.